Tracking transmitter-gated P2X cation channel activation *in vitro* and *in vivo*

Esther Richler[1,4], Severine Chaumont[1,4], Eiji Shigetomi[1,4], Alvaro Sagasti[3] & Baljit S Khakh[1,2]

We present a noninvasive approach to track activation of ATP-gated P2X receptors and potentially other transmitter-gated cation channels that show calcium fluxes. We genetically engineered rat P2X receptors to carry calcium sensors near the channel pore and tested this as a reporter for $P2X_2$ receptor opening. The method has several advantages over previous attempts to image P2X channel activation by fluorescence resonance energy transfer (FRET): notably, it reports channel opening rather than a conformation change in the receptor protein. Our FRET-based imaging approach can be used as a general method to track, in real time, the location, regional expression variation, mobility and activation of transmitter-gated P2X channels in living neurons *in vitro* and *in vivo*. This approach should help to determine when, where and how different receptors are activated during physiological processes.

The cation selective superfamily of ionotropic receptors, comprising the Cys-loop, glutamate and P2X receptor families[1], collectively underlie excitatory fast synaptic transmission at most synapses in the nervous system. Thus it would be informative to measure activation of specific ionotropic receptors in defined cell types in real time and with micrometer-scale precision. We present a generally applicable approach that achieves these goals for P2X receptors.

The role of ATP signaling in the nervous system is well established[2,3]. We focused on ATP-gated P2X receptors because they are the least understood ionotropic receptors[4]. P2X receptors comprise a family of seven subunits ($P2X_1$–$P2X_7$), several of which are expressed in neurons[3,5]. Mice expressing genetically altered P2X subunits (including $P2X_2$) show defects in nervous system function[3–5]. Ideally, it would be useful to be able to image neurons (or a network) to 'see' where $P2X_2$ receptors are, to 'see' how their density varies, and to 'see' when the receptors are activated. The first two possibilities can be achieved by using genetically encoded optical tags such as GFP[6,7], but so far there has not been a method to image activation of P2X receptors. We therefore sought to develop a single approach that achieves all three aims. Our previous attempt to measure $P2X_2$ receptor activation by FRET provided readouts of a conformational change, but was unsuitable for imaging receptor activation[8]. The approach that we report here overcomes those limitations.

The pores of transmitter-gated cation channels, including P2X, show permeability to Ca^{2+} ions during channel opening[1,9]. Inspired by work on *Drosophila* neuromuscular junctions[10], Na^+ pumps[11] and Ca^{2+} channels[12], we made use of this feature in designing a genetically encoded method for imaging P2X receptor activation. Three advances have made our work on P2X channels feasible. First, the development of genetically encoded FRET-based Ca^{2+} sensors[13,14] has made it possible to image Ca^{2+} fluxes in a genetically encoded manner. Second, nanodomain Ca^{2+} entry through muscle nicotinic channels[15] has been measured with an organic Ca^{2+} indicator dye with an affinity of $\sim$3 μM. Third, the fraction of the current carried by Ca^{2+} in P2X receptors is $\sim$3–14% (ref. 9), which is similar to that in muscle nicotinic channels[15]. On the basis of these data, we considered that the fusion of Ca^{2+} sensors, with affinity in the micromolar range, onto tolerant positions of the $P2X_2$ receptor cytosolic domain would allow optical readouts of activation. Our data show that P2X receptor activation and location can be imaged with FRET microscopy *in vitro* and *in vivo*.

RESULTS

$P2X_2$-cam receptors are functional

We engineered $P2X_2$ receptors to carry genetically encoded YC3.1 tags ($P2X_2$-cam; **Fig. 1a**), which can be used to measure relatively large Ca^{2+} transients that are above background[16]. The Ca^{2+} affinity of YC3.1 at $\sim$2 μM is close to that of the organic Ca^{2+} indicator dye Fluo-4 dextran, which has been used to image Ca^{2+} entry through nicotinic channels[15,16]. We reasoned that indicators with micromolar Ca^{2+} affinity would be ideal because only 3–14% of the P2X current is carried by Ca^{2+}. YC3.1 was fused to the carboxy (C) terminus of $P2X_2$ (ref. 17). YC3.1 contains cyan fluorescent protein (CFP) and yellow fluorescent protein (YFP) separated by a Ca^{2+} sensor domain, which undergoes a conformational change on Ca^{2+} binding, altering CFP-YFP proximity and resulting in an increase in FRET[13,14]. For initial characterization, we expressed $P2X_2$-cam receptors in human embryonic kidney (HEK) 293 cells (**Fig. 1**). We observed strong YFP and CFP fluorescence for $P2X_2$-cam

[1]Department of Physiology and [2]Department of Neurobiology, David Geffen School of Medicine, and [3]Department of Molecular, Cellular and Developmental Biology, University of California Los Angeles, 10833 LeConte Avenue, Los Angeles, California 90095, USA. [4]These authors contributed equally to this work. Correspondence should be addressed to B.S.K. (bkhakh@mednet.ucla.edu).

RECEIVED 25 SEPTEMBER; ACCEPTED 13 NOVEMBER; PUBLISHED ONLINE 16 DECEMBER 2007; DOI:10.1038/NMETH1144

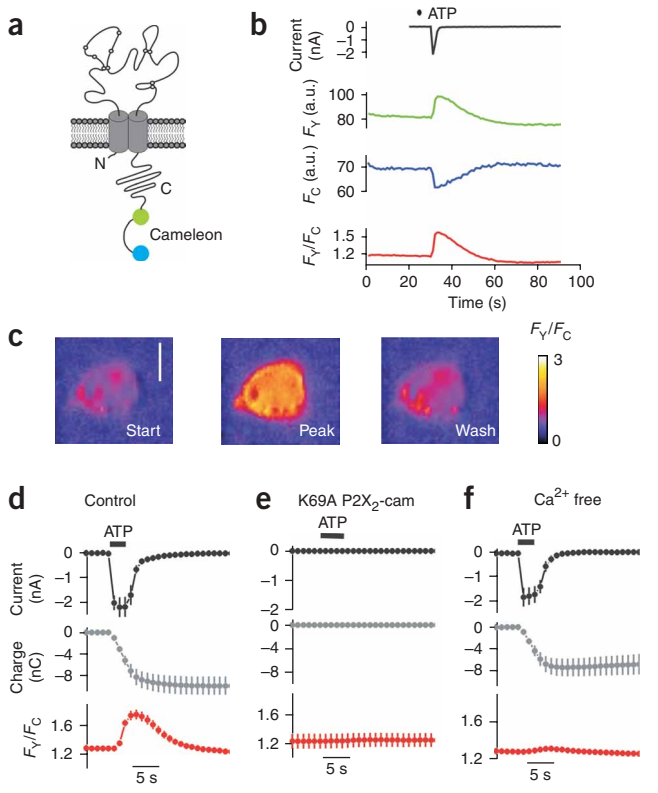

Figure 1 | $P2X_2$-cam receptors are functional and show ATP-evoked FRET changes. (**a**) $P2X_2$ subunit with YC3.1 attached on the C-terminal tail to form $P2X_2$-cam. (**b**) Representative traces of ATP-evoked membrane currents and changes in F_Y, F_C and F_Y/F_C. (**c**) Representative FRET (F_Y/F_C) images of HEK cells before, during and after ATP application. Scale bar, 10 μm. (**d–f**) Traces showing the holding current (top), the integral of the current (middle) and the change in F_Y/F_C (bottom) in HEK cells before, during and after ATP application for wild-type channels (**d**), channels with K69A mutations that disrupt ATP binding (**e**), and cells expressing $P2X_2$-cam channels bathed in Ca^{2+}-free solutions (**f**).

receptors that localized to the plasma membrane and no evidence of protein degradation (**Supplementary Fig. 1a,b** online).

$P2X_2$-cam receptors were functional and their ATP-evoked currents were similar to those of wild-type $P2X_2$. For wild-type $P2X_2$, the effective concentration for half-maximum response (EC_{50}) and Hill slope for the ATP concentration-response were 12 ± 2 μM (negative logarithm of EC_{50} (pEC_{50}) = −5.0 ± 0.08) and 1.9 ± 0.2 (n = 13; **Supplementary Fig. 1c**). For $P2X_2$-cam receptors, they were 14 ± 2 μM (pEC_{50} = −4.9 ± 0.05) and 2.0 ± 0.2 (n = 9; $P > 0.05$ for pEC_{50} values by Student's unpaired t-test). The peak current densities for $P2X_2$-cam receptors tended to be larger than those for wild-type $P2X_2$ (−293 ± 50 and −190 ± 20 pA/pF, respectively; P = 0.04). Thus, overall there were no functional deficits in $P2X_2$-cam receptors. We also verified that $P2X_2$-cam receptors were permeable to Ca^{2+} (**Supplementary Methods** online). The ratio of Ca^{2+} to Cs^+ permeability (pCa^{2+}/pCs^+) for $P2X_2$-cam receptors and wild-type $P2X_2$ receptors was not significantly different (2.7 ± 0.4 (n = 7) and 3.7 ± 0.2 (n = 5), respectively; P = 0.08, Student's unpaired t-test), and consistent with past measurements[5]. The FRET efficiency of YC3.1 in $P2X_2$-cam was also similar to previous estimates[8] (24.5 ± 0.6%, n = 12; **Supplementary Fig. 2** online).

FRET for $P2X_2$-cam reports receptor activation in HEK cells

We made whole-cell patch-clamp recordings from HEK cells while simultaneously recording YFP and CFP emission with a custom setup[8] (**Supplementary Fig. 3** online) to determine whether FRET changes occurred during receptor activation (**Fig. 1b**). We plotted whole-cell currents, YFP (F_Y) and CFP (F_C) intensities, and the ratio of YFP to CFP intensity (F_Y/F_C) over time (**Fig. 1b**). On ATP application, we recorded inward currents, an increase in F_Y, a decrease in F_C and an increase in the F_Y/F_C ratio indicative of an increase in FRET (**Fig. 1b**). These changes were readily observable by eye from the images of F_Y and F_C, and from the F_Y/F_C traces (**Fig. 1b,c**).

We determined whether some of the ATP-evoked FRET signal (**Fig. 1b**) was contaminated by changes taking place inside the cell, such as changes due to global increases in Ca^{2+}. First, we repeated the FRET experiments by combining FRET with total internal reflection fluorescence (TIRF) microscopy (**Supplementary Fig. 4** online). We found that the F_Y/F_C changes were almost identical between epifluorescence and TIRF microscopy (36 ± 3 (n = 10) and 37 ± 3% (n = 15), respectively), indicating that channels in the plasma membrane show increased FRET in response to ATP. Second, we found that the $P2X_2$-cam FRET signals were not simply due to increases in global Ca^{2+}, because the FRET and global Ca^{2+} signal kinetics were distinct, and because an increase in global Ca^{2+} in the cells did not lead to an increase in FRET for $P2X_2$-cam (**Supplementary Note 1** online). In addition, using FRET between CFP and YFP attached to the amino (N) and C termini of the $P2X_2$ receptor, we estimated that the distance between the C tail tip (where YC3.1 was attached) and the inner aspect of the pore was ~6 nm. Thus, the YC3.1 moiety was attached to $P2X_2$ receptors in a nanodomain (**Supplementary Note 2** online).

To explore the relationship between FRET and ATP-evoked currents, we compared the time course of the inward currents to the change in F_Y/F_C and to total charge transfer[9] obtained by integrating the currents (expressed in Coulombs; **Fig. 1d**). Application of ATP evoked a robust increase in FRET with a time course similar to the ATP-evoked current (**Fig. 1d**). Both ATP-evoked currents and FRET signals were absent in $P2X_2$-cam receptors carrying K69A mutations (**Fig. 1e**) that disrupt ATP binding[18], ruling out any detectable contribution of endogenous P2Y receptors to the responses. By contrast, only the FRET changes were abolished in cells bathed in nominally Ca^{2+}-free extracellular solutions (**Fig. 1f**). Overall, these data indicate that the FRET increases are due to ATP activation of $P2X_2$-cam receptors themselves and to Ca^{2+} flow through the pore.

FRET for all homomeric P2X receptors

We tagged all P2X subunits with Ca^{2+} sensors to determine whether F_Y/F_C changes could be recorded in response to ligand activation for all homomeric receptors, (**Supplementary Fig. 5** online). We detected robust F_Y/F_C changes for all homomeric P2X receptors with the exception of nonfunctional $P2X_6$ channels[5]. For a specific set of experiments, the F_Y/F_C changes (%) were $P2X_1$, 7 ± 2% (n = 7); $P2X_2$, 43 ± 2% (n = 6); $P2X_3$, 10 ± 3% (n = 5); $P2X_4$, 34 ± 3% (n = 6); $P2X_5$, 5 ± 1% (n = 6); $P2X_6$, 1 ± 0.4% (n = 4); and $P2X_7$, 9 ± 2% (n = 4). In comparison, the fractional Ca^{2+} currents for these channels are 12, 6, 3, 11, 5, 0 and 5%, respectively[9], values that span those of many nonselective cation

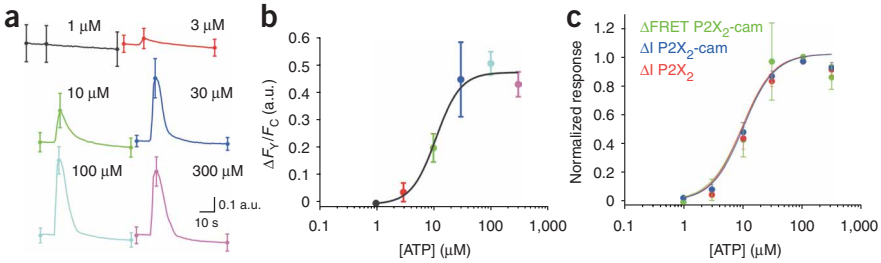

Figure 2 | Concentration-dependent ATP-evoked FRET changes for $P2X_2$-cam channels expressed in HEK cells. (**a**) Representative F_Y/F_C traces for puff application of the indicated ATP concentrations. (**b**) Concentration-response curves for ATP-evoked changes in F_Y/F_C. (**c**) Normalized concentration-response curves for ATP-evoked changes in F_Y/F_C, currents for $P2X_2$-cam receptors and currents for wild-type $P2X_2$ receptors.

channels including AMPA, nicotinic, 5HT3, NMDA and TRP receptor channels[9]. Thus, FRET imaging with Ca^{2+} sensor tags may be useful for imaging the activation of nonselective cation channels in general.

Comparison of FRET imaging with electrophysiology

The standard method for measuring transmitter-gated ion channel responses is whole-cell patch-clamp recording. We directly compared patch-clamp recordings of ATP-evoked inward currents and FRET signals for our reporter (**Fig. 2** and **Supplementary Fig. 6** online). The normalized data indicated that the EC_{50} (10 μM) and Hill slope (~2) values were indiscernible from those for ATP-evoked current measurements at $P2X_2$-cam or wild-type $P2X_2$ receptors measured with patch-clamp recording (**Fig. 2b**,**c**). In addition, the duration and rundown of the FRET responses followed those of the ATP-evoked current (**Supplementary Fig. 6**). These data suggest that $P2X_2$-cam receptor activation can be tracked by FRET with response profiles and ATP sensitivity similar to those recorded by whole-cell patch-clamp recording.

$P2X_2$-cam receptors in hippocampal neurons

We expressed $P2X_2$-cam receptors in hippocampal neurons, where native $P2X_2$ receptors are also found[19,20]. We observed strong yellow and cyan fluorescence throughout the somatodendritic compartment, including in fine filopodia and in distal dendrites up to >100 μm away from the soma (**Fig. 3a**). The fluorescence was strongly localized at the membrane, and there were hotspot regions along the dendrites[20] (**Fig. 3a**,**b**).

We measured fluorescence recovery after photobleaching (FRAP) of $P2X_2$-cam in somatic and dendritic regions of hippocampal neurons (**Fig. 3c**) to estimate the average mobility of $P2X_2$-cam receptors[21] (**Fig. 3d**). There was a significant difference in the FRAP time constants between somatic and dendritic regions: $P2X_2$-cam receptors moved 30% slower in the hippocampal neuron somata than in the dendrites ($P < 0.01$; **Fig. 3e**). The estimated diffusion coefficients (D) of $P2X_2$ receptors were ~0.02 and ~0.01 μm²/s, implying that the receptors would diffuse ~0.2 and ~0.14 μm in ~1 s in one dimension in the dendritic and somatic regions, respectively. These values of D are consistent with those generally expected for membrane proteins[21]. The difference in mobility between somatic and dendritic regions emphasizes a useful feature of $P2X_2$-cam: namely, because each $P2X_2$ receptor carries three YC3.1 tags, intrinsic fluorescence can be used to track the regional variation and mobility of the receptors.

$P2X_2$-cam receptor activation in hippocampal neurons

We measured the FRET efficiency of $P2X_2$-cam receptors in hippocampal neurons (**Supplementary Fig. 7** online) and found that it was close to that in HEK cells (21.5 ± 1.4% for somata, $n = 11$; 19.4 ± 2.4% for dendrites, $n = 7$). We then determined whether ATP evoked changes in FRET from neurons expressing $P2X_2$-cam. We puffed 100 μM ATP for ~1–3 s to the soma or dendrites and measured increases and decreases in F_Y and F_C, respectively (**Fig. 4a–d**). Thus, $P2X_2$-cam channels are functional in hippocampal neurons, and their activation can be tracked in spatially distinct neuronal compartments.

The magnitude of the FRET change in response to ATP in neuron somata was similar to that in HEK cells (**Fig. 4e**). In dendrites, the signal was smaller but statistically significant (**Fig. 4e**;

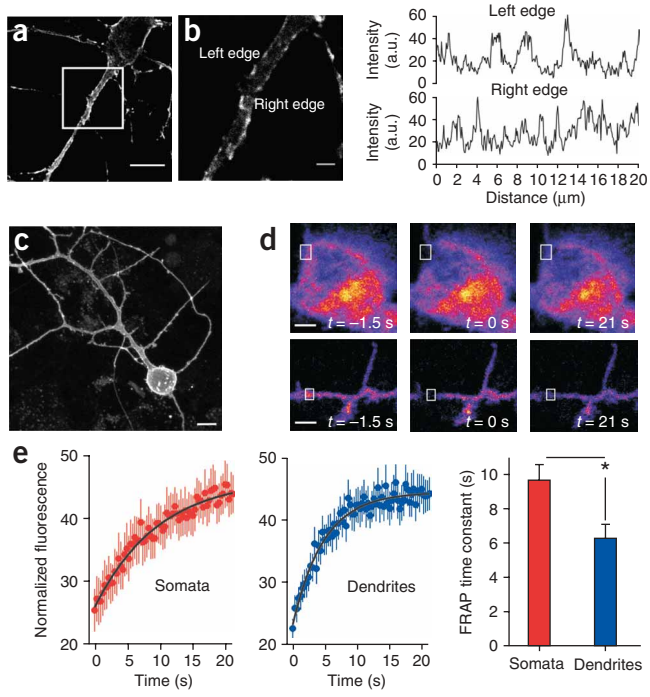

Figure 3 | $P2X_2$-cam is targeted to the plasma membrane of hippocampal neurons and can move to recover from photobleaching. (**a**) Confocal image of a hippocampal neuron expressing $P2X_2$-cam receptors. (**b**) Left, magnification of the boxed region in **a**; note localization of the fluorescence at the membrane of the soma and dendrites. Right, line profiles along the left and right edge of the dendrite shown on the left; note the hotspot regions of high density. (**c**) Images of hippocampal neurons expressing $P2X_2$-cam to illustrate the broad somatodendritic expression pattern. (**d**) Top, images of a hippocampal neuron soma before, during and after photobleaching of a small region of interest (box). Bottom, the same experiment shown for dendritic regions. (**e**) FRAP curves for somatic ($n = 11$) and dendritic ($n = 22$) regions, and average time constants for FRAP. For the FRAP recovery graphs, the y axis indicates fluorescence intensity as a percentage of the prebleach control value ($T = -1.5$ s). Scale bars, 10 μm (**a**,**c**); 2 μm (**b**).

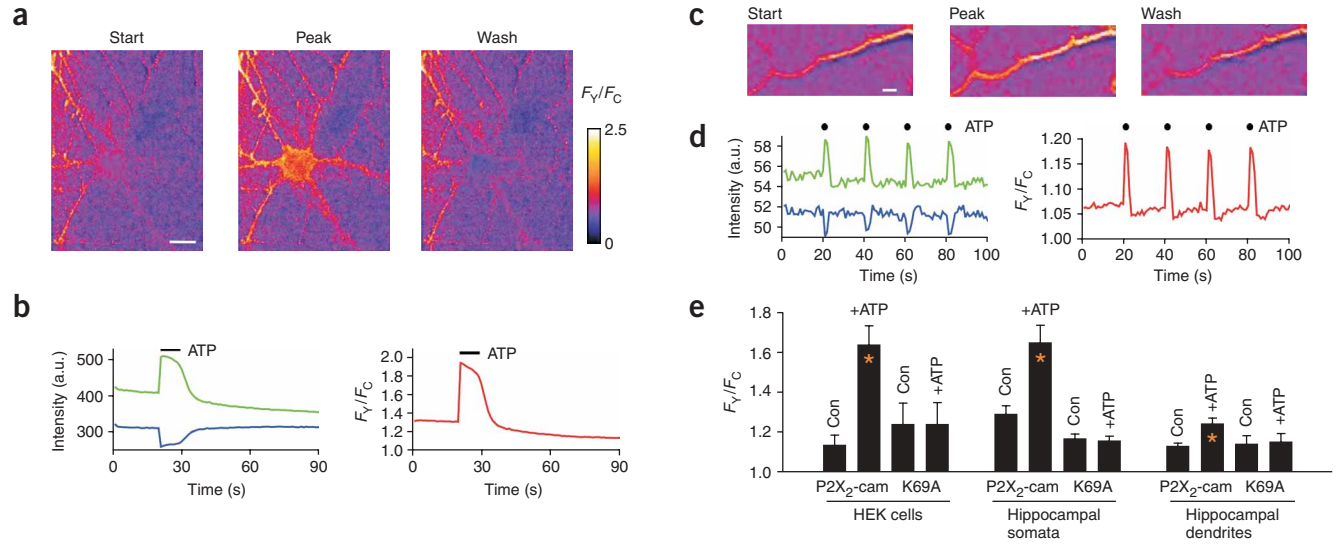

Figure 4 | ATP-evoked FRET changes for $P2X_2$-cam channels expressed in hippocampal neurons. (**a**,**b**) Representative FRET images (**a**) and data (**b**) before, during and after ATP application to hippocampal somata. (**c**,**d**) Representative FRET images (**c**) and data (**d**) before, during and after ATP application to hippocampal dendrites. (**e**) Summary of data for the experiments represented in **a**–**d**; data from HEK cells are included for comparison. Error bars, s.e.m. FRET changes were not observed for K69A mutants. The control (con) was the F_Y/F_C value before ATP application. Scale bars, 10 μm (**a**); 2 μm (**c**).

$P < 0.05$). We observed no changes in F_Y or F_C in hippocampal neurons expressing K69A $P2X_2$-cam, which is deficient in ATP binding[18] (**Fig. 4e**). Thus, the FRET responses represent activation of $P2X_2$-cam receptors rather than an unknown ATP-triggered mechanism. The K69A mutant $P2X_2$-cam receptors are valuable controls because they indicate that spontaneous neuronal Ca^{2+} changes do not contribute to the FRET signal.

Endogenous ATP release from hippocampal neurons

Because ATP is released from hippocampal neurons during electrical stimulation of afferent fibers[22] and by synaptic transmission[23,24], we tested the possibility that $P2X_2$-cam receptors may report receptor activation in hippocampal neurons. We monitored F_Y, F_C and F_Y/F_C traces over a 300-s time window ($n = 20$) and found no evidence for changes in any of these parameters, suggesting that under resting conditions insufficient ATP is released to activate $P2X_2$-cam receptors, a finding that is consistent with the rarity[4] of spontaneous P2X-mediated excitatory postsynaptic currents. We used electrical field stimulation (EFS) of hippocampal neurons to evoke transmitter release in culture[25]. We began by applying 90 action potentials in a 3-s window and plotting the change in F_Y/F_C from neurons expressing $P2X_2$-cam receptors (**Fig. 5**). Increases in FRET were measured in all neurons ($n = 26$) for more than three action potentials (**Fig. 5c**). We therefore used 90 action potentials as a reproducible and robust signal to probe further the nature of the FRET signal.

We explored the possibility that FRET signals represent the release of endogenous ATP (**Fig. 5a**,**b**). First, we repeated the

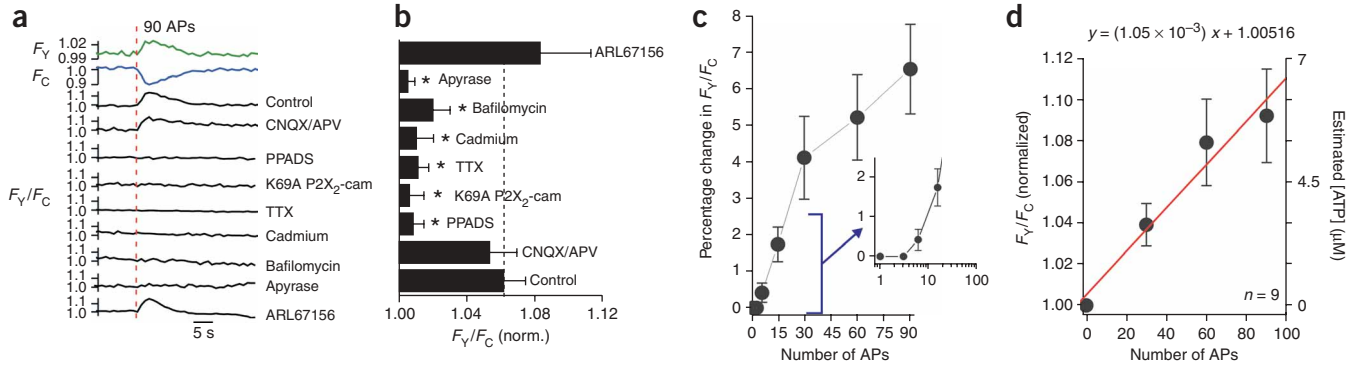

Figure 5 | Activation of $P2X_2$-cam receptors by endogenous ATP in hippocampal neurons. (**a**) Representative YFP and CFP traces (green and blue) and F_Y/F_C traces under the indicated conditions. At the indicated time point (red line), 90 action potentials (APs) were triggered in 3 s, resulting in FRET changes in some of the traces. (**b**) Summary of data from 4–21 experiments. Asterisks indicate significant ($P < 0.05$) reductions in the F_Y/F_C signal. The concentration of each drug is given in the text. (**c**) Relationship between action potential number and percentage change in F_Y/F_C. Inset shows the initial phase on a log scale for the *x* axis; note that there was no FRET change for fewer than nine action potentials. (**d**) Relationship between the change in F_Y/F_C and the number of action potentials applied. The red line is a linear fit of the equation shown above the graph. The right green axis shows the estimated ATP concentration needed to trigger an equivalent FRET response on the basis of the dose-response curves shown in **Figure 2c**.

experiments with inhibitors of AMPA (CNQX) and NMDA (APV) receptors in the bath (30 μM; $n = 6$). These inhibitors did not reduce the $P2X_2$-cam FRET signal in response to EFS, indicating that Ca^{2+} entry through glutamate channels contributes little to the measured signal. FRET changes were, however, completely blocked by the P2X antagonist PPADS[3] (10 μM; $n = 5$), and were not observed in neurons expressing K69A $P2X_2$-cam receptors ($n = 5$; **Fig. 5a**,**b**). These data suggest that the EFS evoked $P2X_2$-cam FRET signal is due to endogenous ATP release. We also used TTX (250 nM; $n = 5$) and Cd^{2+} (30 μM; $n = 4$) to block voltage-dependent Na^+ and Ca^{2+} channels, respectively, and found that the FRET change was largely reduced (**Fig. 5a**,**b**), implying that EFS causes action potential firing and Ca^{2+} channel–dependent ATP release from nerve terminals[3,5].

To test this possibility further, we used bafilomycin, an inhibitor of vesicular transmitter release. If the EFS-evoked FRET change were due to vesicular ATP, then bafilomycin should block it. Indeed, we observed no significant EFS-evoked increases in F_Y/F_C in the presence of bafilomycin ($n = 5$; **Fig. 5a**,**b**). We also tested the effect of apyrase, because if the EFS-evoked F_Y/F_C signals were due to endogenous ATP, then this ATPase should degrade ATP and thus decrease the FRET signal. Consistent with this idea, we observed negligible F_Y/F_C changes in the presence of apyrase (10 U/ml; $n = 6$; **Fig. 5a**,**b**). We also determined whether endogenous ectoATPases shaped the EFS-evoked FRET signal by testing the actions of ARL67156, an ectoATPase inhibitor (30 μM; **Fig. 5a**,**b**). In the presence of ARL67156, the FRET signals tended to be larger but did not reach statistical significance (**Fig. 5a**,**b**), suggesting that endogenous ectoATPases contribute little to the FRET responses. These pharmacological experiments indicate that EFS may evoke the release of vesicular ATP, which binds to $P2X_2$-cam receptors to cause FRET changes. Thus, the change in F_Y/F_C is not observed in the presence of PPADS or for K69A $P2X_2$-cam receptors, and is sensitive to TTX, Cd^{2+}, bafilomycin and apyrase (**Fig. 5b**).

We next analyzed the rising phase of the EFS-evoked F_Y/F_C change under control conditions (**Fig. 5d**) to determine whether the concentration of ATP experienced by open $P2X_2$-cam receptors could be estimated. We plotted the F_Y/F_C change versus the number of action potentials, and estimated the ATP concentration on the basis of the ATP dependence of the FRET signal shown in **Figure 2c** (**Fig. 5d**). These experiments suggest that the relationship between F_Y/F_C and action potentials is linear up to 90 action potentials, predicting that one action potential evokes a negligible change in FRET (<0.5%). In addition, the data and analysis suggest that 30–90 action potentials give rise to FRET signals equivalent to those triggered by ~3–6 μM ATP, implying that the amount of ATP liberated during action potential firing is small and below the level expected to saturate postsynaptic P2X receptors.

Sensory neuron expression and receptor activation *in vivo*

P2X subunits are expressed in zebrafish somatosensory neurons[26–31]. At early stages of development, $P2X_3$ orthologs predominate in sensory neurons of zebrafish[30,31], but $P2X_2$ orthologs also exist at later developmental stages[32]. We cloned a putative promoter for the gene encoding $P2X_3$ from the pufferfish *Fugu* and used it to drive expression of the GAL4-VP16 transcription factor (**Supplementary Fig. 8** online), which in turn induced expression of $P2X_2$-cam, cytosolic GFP or K69A $P2X_2$-cam receptors in zebrafish peripheral sensory neurons *in vivo*[30,31]. Fluorescence was observed in both sensory trigeminal ganglion and Rohon-Beard (RB) neurons[31]. We subsequently focused on the RB neurons, which are the functional equivalents of dorsal root ganglion neurons in zebrafish at early stages of development. Initially, we compared the expression of GFP in RB neurons[30,31]. $P2X_2$-cam receptors were readily observable but showed less intense fluorescence than cytosolic GFP in RB neuron somata and neurites (**Supplementary Fig. 8**). We visually examined 20 images of $P2X_2$-cam– and GFP-expressing RB neurons, and found that the overall expression pattern, location and morphology of neurons were indistinguishable[33] (see **Supplementary Fig. 8** for two examples of each). We conclude that the *Fugu* $P2X_3$ promoter drives the expression of $P2X_2$-cam and GFP in a common set of RB neurons, and that $P2X_2$-cam expression does not alter the morphology of these neurons.

We measured FRET for $P2X_2$-cam receptors in RB neurons *in vivo* and found that the FRET efficiency was 20 ± 3% ($n = 6$; **Fig. 6a**,**b**), which was not significantly different to our earlier measurements in HEK cells or in hippocampal neuron somata or dendrites ($P > 0.05$; Tukey's one-way analysis of variance). We then used a patch-pipette filled with 100 μM ATP, positioned within 100 μm of fluorescent RB neurons, to puff on ATP with a picospritzer, and imaged F_Y, F_C and F_Y/F_C over time with a

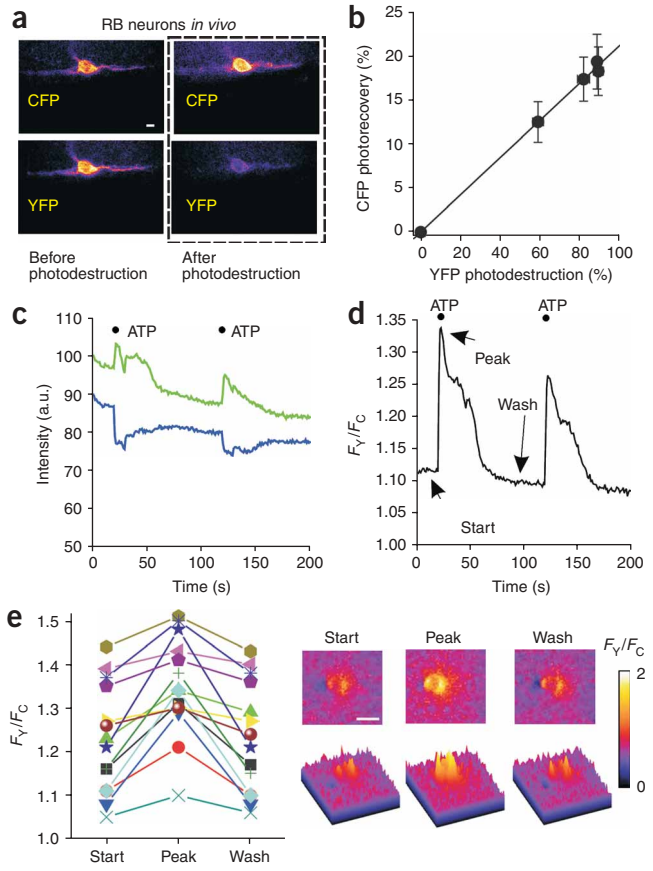

Figure 6 | *In vivo* FRET experiments for $P2X_2$-cam channels. (**a**,**b**) Representative images and plot of FRET efficiency of $P2X_2$-cam receptors in RB neurons *in vivo*. (**c**,**d**) Fluorescence intensity and F_Y/F_C data for ATP-evoked FRET changes for $P2X_2$-cam receptors in RB neurons. (**e**) Left, scatter graph showing data from all fish that did not move. Right, FRET images of the ATP-evoked changes. Scale bars, 10 μm (**a**,**e**).

beam splitter (**Supplementary Fig. 3**). On application of ATP, we observed ratiometric changes in YFP and CFP fluorescence and robust increases in F_Y/F_C (see the example in **Fig. 6c,d**, and the scatter graph of 14 fish and images in **Fig. 6e**). In relation to the data obtained in HEK cells and hippocampal neurons, the *in vivo* data were more variable, perhaps because of movement of the zebrafish. We did not detect ratiometric FRET changes in RB neurons expressing $P2X_2$-cam receptors in response to puff applications of buffer alone ($n = 17$), or in RB neurons expressing K69A $P2X_2$-cam receptors in response to ATP application ($n = 34$). These experiments suggest that $P2X_2$-cam reports receptor activation *in vivo*, and that the method can be extended to all P2X receptors in zebrafish owing to the favorable optical qualities of this organism[26–31].

DISCUSSION

We have shown that a FRET-based imaging approach can be used to track the location, regional expression, mobility and activation of transmitter-gated P2X channels *in vitro* and *in vivo*.

The characterization and proof-of-principle experiments show that our approach is a manifest improvement on previous FRET-based attempts to image P2X activation[8]. This approach can now be used to understand the conditions under which ATP is released, which dendrites of a neuron are activated by endogenous ATP, where P2X receptors are activated on dendrites, whether ATP signaling varies between the soma and dendrites, how much ATP is released during action potential firing, and how quickly P2X receptors move. Much can also be learned by using GFP-tagged channels and Ca^{2+} indicator dyes. With our reporter, however, we can measure the location, mobility and activation of P2X receptors with a single genetically encoded protein and without perturbing Ca^{2+} buffering in the neuron, as occurs with organic Ca^{2+} dyes. We also gain spatial resolution that is not possible with electrophysiology. Lastly, because the reporter is attached to the P2X channel itself, the signal is measured in a nanodomain near the pore. In the future, it may be possible to improve our approach by using tetracysteine-reactive Ca^{2+} indicator dyes[12].

We chose a FRET-based system because the measurements are ratiometric, which minimized artifacts arising from out-of-focus light[13]. This feature is desirable for experiments in complex cellular systems such as neurons and whole organisms. Single-wavelength systems may be equally as useful. In addition, fluorescent proteins are continually being improved by redesign and mutagenesis, and in future work the modular design of our constructs may be useful for determining the utility of new generations of fluorescent proteins[13,14]. The approach that we report works for all functional homomeric P2X receptors. We did not study heteromeric P2X receptors because a mixture of trimeric channel receptors is expected when any two P2X subunits are expressed, and we have not devised a method to isolate the optical signals from the different channel populations.

$P2X_2$ receptors tagged on the cytosolic C-terminal domain with the genetically encoded Ca^{2+} sensor YC3.1 functioned in a manner almost identical to wild-type P2X receptors[34]. ATP evoked both inward currents and F_Y/F_C changes for the attached YC3.1 protein module within a nanodomain of the inner mouth of the pore[14]. The strong subunit-specific nature of the FRET signal, the kinetic differences between FRET and global Ca^{2+} signals, and the fact that comparable global Ca^{2+} changes did not result in FRET signals together suggest that the signal that we report for $P2X_2$ receptors is due to Ca^{2+} entry through the $P2X_2$ receptor pores themselves. Thus, by virtue of covalent attachment, FRET-based measurements report on biologically relevant activity in volumes and domains appropriate to the size of single receptors and/or channels. Our work thus builds on previous pioneering work on Na^+ pumps[11] and voltage-dependent Ca^{2+} channels[12], extending it to transmitter-gated P2X receptors[15].

The data obtained with the K69A mutant and Ca^{2+}-free solutions strongly suggest that the FRET changes resulted from Ca^{2+} entry through the $P2X_2$ pore, but the kinetics were sluggish as compared with the current. In direct comparisons, for example, the decay time (τ) for FRET was $\sim$6 s, whereas the τ value for the current was $\sim$2.5 s (**Fig. 1d**). This difference probably represents the interaction kinetics of Ca^{2+} with the reporter. The FRET kinetics may represent a limitation of the approach for imaging the time course of fast ATP synaptic responses, and it may be necessary to optimize the reporter to track the time course of fast synaptic events[12,14].

The mutant K69A $P2X_2$-cam served as a vital and necessary control; Lys69 is an important site for ATP recognition[4], and K69A receptors are not likely to bind ATP and therefore cannot be activated. Thus, by comparing responses recorded from neurons expressing K69A $P2X_2$-cam and those expressing wild-type $P2X_2$-cam receptors, it is possible to rule out the contribution of non-$P2X_2$ receptor–mediated Ca^{2+} signals, such as those mediated by metabotropic ATP receptors or other sources of intracellular Ca^{2+}. In future studies, it will be important to ensure that any measured FRET responses are indeed due to Ca^{2+} entry through P2X receptors by comparing the signals to those measured with K69A mutants. Thus, in experiments using this reporter, it should be concluded that a signal is mediated by ATP acting on the P2X-cam receptors themselves only when a FRET signal is absent in parallel measurements with K69A $P2X_2$-cam.

The study of ATP signaling and P2X receptors is an infant field with several important unresolved issues[5], some of which can now be addressed with our reporter. First, an outstanding issue is the pathophysiological conditions under which P2X receptors are activated. $P2X_2$-, $P2X_3$- and $P2X_4$-cam receptors introduced into neurons through viral infection of the target cells, through transgenic expression or through gene targeting could be used to study this issue. For example, they could be used to study P2X activation in pain[5] and sound transduction[35]. Second, much of our understanding of P2X receptor biophysics is based on hypothesis-driven mutagenesis[18]. Although substantial progress has been made[18], a mechanistic understanding of the ATP-binding site and pore remains a goal of the field. Because $P2X_2$-cam receptors can be studied by imaging with the same sensitivity as whole-cell patch-clamp recording, it may be possible to use a random mutagenesis approach to shed light on how P2X receptors work. Last, P2X receptors are emerging as important drug targets for pain and inflammation[4]. Thus, stable cell lines expressing each of the P2X-cam receptors could be used for FRET-based high-throughput screening of chemical libraries for subunit-specific agonists and antagonists.

METHODS

FRET microscopy. For most of the experiments, we used an Olympus BX50 microscope equipped with a Peltier-cooled (−15 °C), Imago CCD camera (640 × 480 pixels; each pixel, 9.9 × 9.9 μm),

epifluorescence condenser, control unit (containing ISC and PDC boards) and Polychrome IV (TILL Photonics). The hardware was controlled by a personal computer, an appropriate frame grabber (TILL Photonics) and macros driven by TILLvisION v3.3 software. The cells were viewed with a ×40 water immersion objective lens with a numerical aperture of 0.8 (Olympus). We used the following filters for acquiring CFP or YFP images (order is dichroic, emitter in nm): CFP (455DRLP, 480AF30) and YFP (525DRLP, 545AF35; all from Glen Spectra). For photodestruction of YFP, we used 525-nm light from the monochromator and a 525 DRLP dichroic filter. F_Y/F_C changes over time were recorded with a beam splitter (Cairn Optosplit) inserted in the emission path of the microscope (**Supplementary Fig. 3**). Our use of zebrafish embryos was approved by the University of California Los Angeles Chancellors Animal Research Committee.

Additional methods. Descriptions of the molecular biology, HEK 293 cell culture, immunoblotting, patch-clamp electrophysiology, FRAP, TIRF microscopy, hippocampal cell culture, neuron transfection, molecular biology and imaging of zebrafish, agonist applications, electrical field stimulation, data analysis, software and statistical analysis are given in **Supplementary Methods**.

Note: Supplementary information is available on the Nature Methods website.

ACKNOWLEDGMENTS

We thank A.F. Schier (Harvard University) for cloning of the *Fugu* $P2X_3$ enhancer; R.Y. Tsien (University of California San Diego) for providing YC3.1 cDNA; H. Singh and E. Toulme for comments and discussions; J. Fisher for an early version of **Supplementary Figure 3**; and F. Schweizer and G. David for advice on working with hippocampal neurons and reagents. E.R. was supported by a Molecular Cellular Integrative Physiology Predoctoral Fellowship, a Buschwald Fellowship and a Neural Repair Training Grant Predoctoral Fellowship. E.S. was supported by the Uehara Memorial Foundation (Japan). Zebrafish work was supported by a Burroughs-Wellcome Career Award in the Biomedical Sciences to A.S. The laboratory (B.S.K.) was supported by the National Institutes of Health, the Human Frontiers Science Program, the Whitehall Foundation and a Stein/Oppenheimer Endowment Award.

AUTHOR CONTRIBUTIONS

E.R., S.C., E.S. and B.S.K. designed and did the experiments, contributed data, helped to make the figures, and wrote the paper. A.S. contributed laboratory space, made the vectors for the zebrafish work, and helped to make the figures and to write the paper.

Published online at http://www.nature.com/naturemethods/
Reprints and permissions information is available online at http://npg.nature.com/reprintsandpermissions

1. Hille, B. *Ion Channels of Excitable Membranes* 3rd edn (Sinauer Associates, Sunderland, MA, 2001).
2. Burnstock, G. Purinergic nerves. *Pharmacol. Rev.* **24**, 509–581 (1972).
3. Burnstock, G. Physiology and pathophysiology of purinergic neurotransmission. *Physiol. Rev.* **87**, 659–797 (2007).
4. Khakh, B.S. & North, R.A. P2X receptors as cell surface ATP sensors in health and disease. *Nature* **442**, 527–532 (2006).
5. North, R.A. Molecular physiology of P2X receptors. *Physiol. Rev.* **82**, 1013–1067 (2002).
6. Chiu, C.-S., Kartalov, E., Unger, M., Quake, S. & Lester, H.A. Single-molecule measurements calibrate green fluorescent protein surface densities on transparent beads for use with 'knock-in' animals and other expression systems. *J. Neurosci. Methods* **105**, 55–63 (2001).
7. Sugiyama, Y., Kawabata, I., Sobue, K. & Okabe, S. Determination of absolute protein numbers in single synapses by a GFP-based calibration technique. *Nat. Methods* **2**, 677–684 (2005).
8. Fisher, J.A., Girdler, G. & Khakh, B.S. Time resolved measurement of state specific P2X ion channel cytosolic gating motions. *J. Neurosci.* **24**, 10475–10487 (2004).
9. Egan, T.M. & Khakh, B.S. Contribution of calcium ions to P2X channel responses. *J. Neurosci.* **24**, 3413–3420 (2004).
10. Guerrero, G. *et al.* Heterogeneity in synaptic transmission along a *Drosophila* larval motor axon. *Nat. Neurosci.* **8**, 1188–1196 (2005).
11. Lee, M.Y. *et al.* Local subplasma membrane Ca^{2+} signals detected by a tethered Ca^{2+} sensor. *Proc. Natl. Acad. Sci. USA* **103**, 13232–13237 (2006).
12. Tour, O. *et al.* Calcium Green FlAsH as a genetically targeted small-molecule calcium indicator. *Nat. Chem. Biol.* **3**, 423–431 (2007).
13. Miyawaki, A. Innovations in the imaging of brain functions using fluorescent proteins. *Neuron* **48**, 189–199 (2005).
14. Palmer, A.E. & Tsien, R.Y. Measuring calcium signaling using genetically targetable fluorescent indicators. *Nat. Protoc.* **1**, 1057–1065 (2006).
15. Demuro, A. & Parker, I. 'Optical patch-clamping': single-channel recording by imaging Ca^{2+} flux through individual muscle acetylcholine receptor channels. *J. Gen. Physiol.* **126**, 179–192 (2005).
16. Miyawaki, A., Griesbeck, O., Heim, R. & Tsien, R.Y. Dynamic and quantitative Ca^{2+} measurements using improved cameleons. *Proc. Natl. Acad. Sci. USA* **96**, 2135–2140 (1999).
17. Khakh, B.S. *et al.* Activation-dependent changes in receptor distribution and dendritic morphology in hippocampal neurons expressing $P2X_2$–green fluorescent protein receptors. *Proc. Natl. Acad. Sci. USA* **98**, 5288–5293 (2001).
18. Egan, T.M., Samways, D.S. & Li, Z. Biophysics of P2X receptors. *Pflugers Arch.* **452**, 501–512 (2006).
19. Kanjhan, R. *et al.* Distribution of the $P2X_2$ receptor subunit of the ATP-gated ion channels in the rat central nervous system. *J. Comp. Neurol.* **407**, 11–32 (1999).
20. Rubio, M.E. & Soto, F. Distinct localisation of P2X receptors at excitatory postsynaptic specializations. *J. Neurosci.* **21**, 641–653 (2001).
21. Lippincott-Schwartz, J., Snapp, E. & Kenworthy, A. Studying protein dynamics in living cells. *Nat. Rev. Mol. Cell Biol.* **2**, 444–456 (2001).
22. Wieraszko, A., Goldsmith, G. & Seyfried, T.N. Stimulation-dependent release of adenosine triphosphate from hippocampal slices. *Brain Res.* **485**, 244–250 (1989).
23. Pankratov, Y., Castro, E., Miras-Portugal, M.T. & Krishtal, O. A purinergic component of the excitatory postsynaptic current mediated by P2X receptors in the CA1 neurons of the rat hippocampus. *Eur. J. Neurosci.* **10**, 3898–3902 (1998).
24. Pankratov, Y.V., Lalo, U.V. & Krishtal, O.A. Role for P2X receptors in long-term potentiation. *J. Neurosci.* **22**, 8363–8369 (2002).
25. Harata, N.C., Aravanis, A.M. & Tsien, R.W. Kiss-and-run and full-collapse fusion as modes of exo-endocytosis in neurosecretion. *J. Neurochem.* **97**, 1546–1570 (2006).
26. Norton, W.H., Rohr, K.B. & Burnstock, G. Embryonic expression of a P2X(3) receptor encoding gene in zebrafish. *Mech. Dev.* **99**, 149–152 (2000).
27. Egan, T.M., Cox, J.A. & Voigt, M.M. Molecular cloning and functional characterization of the zebrafish ATP-gated ionotropic receptor $P2X_3$ subunit. *FEBS Lett.* **475**, 287–290 (2000).
28. Boué-Grabot, E., Akimenko, M.A. & Séguéla, P. Unique functional properties of a sensory neuronal P2X ATP-gated channel from zebrafish. *J. Neurochem.* **75**, 1600–1607 (2000).
29. Diaz-Hernandez, M. *et al.* Cloning and characterization of two novel zebrafish P2X receptor subunits. *Biochem. Biophys. Res. Commun.* **295**, 849–853 (2002).
30. Kucenas, S., Li, Z., Cox, J.A., Egan, T.M. & Voigt, M.M. Molecular characterization of the zebrafish P2X receptor subunit gene family. *Neuroscience* **121**, 935–945 (2003).
31. Kucenas, S., Soto, F., Cox, J.A. & Voigt, M.M. Selective labeling of central and peripheral sensory neurons in the developing zebrafish using $P2X_3$ receptor subunit transgenes. *Neuroscience* **138**, 641–652 (2006).
32. Appelbaum, L., Skariah, G., Mourrain, P. & Mignot, E. Comparative expression of P2X receptors and ecto-nucleoside triphosphate diphosphohydrolase 3 in hypocretin and sensory neurons in zebrafish. *Brain Res.* **1174**, 66–75 (2007).
33. Sagasti, A., Guido, M.R., Raible, D.W. & Schier, A.F. Repulsive interactions shape the morphologies and functional arrangement of zebrafish peripheral sensory arbors. *Curr. Biol.* **15**, 804–814 (2005).
34. Khakh, B.S. *et al.* International Union of Pharmacology. XXIV. Current status of the nomenclature and properties of P2X receptors and their subunits. *Pharmacol. Rev.* **53**, 107–118 (2001).
35. Greenwood, D. *et al.* P2X receptor signaling inhibits BDNF-mediated spiral ganglion neuron development in the neonatal rat cochlea. *Development* **134**, 1407–1417 (2007).